



Improving the Accuracy of Hardness Measurement using UCI Transducers for Inspecting the Heat-Affected Zone of Welded Joints in Steel Pipelines

A. I. Shikhov^a, D. S. Gromyka^{*a}, A. S. Umansky^a, D. V. Kopytina^a, D. R. Shakirzyanova^a, A. M. Shmakov^b

^a Empress Catherine II Saint-Petersburg Mining University, Saint-Petersburg, Russia

^b ITMO University, Saint-Petersburg, Russia

PAPER INFO

Paper history:

Received 17 September 2025

Received in revised form 17 October 2025

Accepted 24 December 2025

Keywords:

Steel Pipes

Weld Seam

Heat-affected Zone

Ultrasonic Contact Impedance

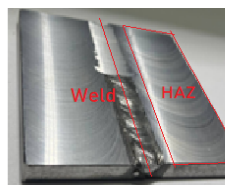
Ultrasonic Wave

Calibration

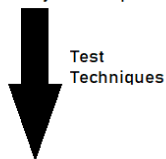
ABSTRACT

Quality control of welded joints involves hardness measurements of both the weld and the heat-affected zone (HAZ). However, standardized hardness testing methods require specimen preparation, leading to pipeline downtime. Among portable devices, hardness testers implementing the Ultrasonic Contact Impedance (UCI) method are the most widely used. However, measurement results depend on the calibration curve, which accounts for the elastic properties of the specimen and assumes their uniformity across the entire inspected surface. In the HAZ of a welded joint, changes in the metal's microstructure and elastic properties occur, leading to measurement errors in UCI hardness testing. This article presents a methodology for applying a correction to the calibration by accounting for actual changes in the elastic modulus within the HAZ, measured via ultrasonic wave velocity monitoring. As a result, hardness values incorporating this correction demonstrated better correlation with reference results obtained using a Vickers microhardness tester, indicating that the proposed correction improves the accuracy of UCI transducer measurements.

doi: 10.5829/ije.2026.39.10a.12



Steel welded joint sample

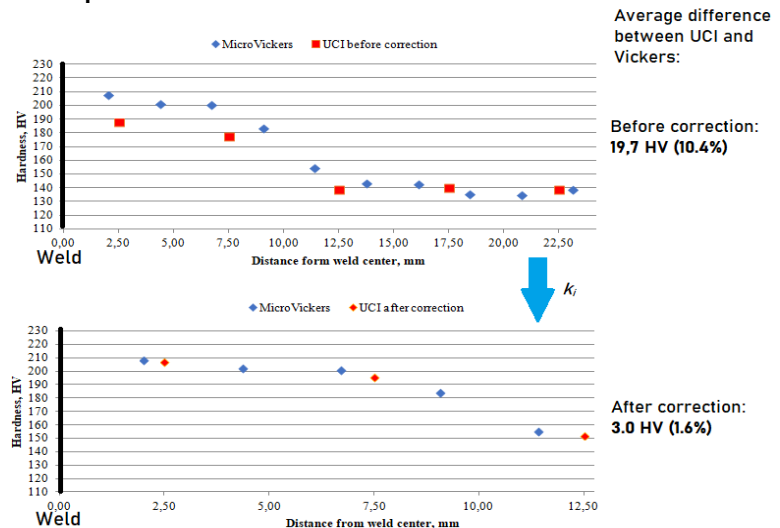


1. Ultrasonic contact impedance (portable device for hardness control)
2. US flaw detector (to measure elastic modulus via US wave speed)
3. MicroVickers (reference method of hardness control)

Correction of UCI using the real elastic modulus with correction factor k :

$$k_t = \frac{E_{real}^t}{E_{calib}}$$

Graphical Abstract



*Corresponding Author Email: Gromyka_DS@pers.spmi.ru (D. S. Gromyka)

Please cite this article as: Shikhov AI, Gromyka DS, Umansky AS, Kopytina DV, Shakirzyanova DR, Shmakov AM. Improving the Accuracy of Hardness Measurement using UCI Transducers for Inspecting the Heat-Affected Zone of Welded Joints in Steel Pipelines. International Journal of Engineering, Transactions A: Basics. 2026;39(10):2500-8.

NOMENCLATURE

HAZ	Heat-affected zone	c_p^2	Longitudinal wave velocity
UCI	Ultrasonic Contact Impedance	E	Elastic modulus, GPa
k_0	Initial stiffness	ν	Poisson's ratios
f	Frequency	HV_{UCI}	Hardness UCI
A_c	Projected contact area of the indenter at the penetration depth	ρ	Density

1. INTRODUCTION

The reliability of gas transportation systems directly depends on the strength of pipeline welded joints (1, 2). According to ISO 9692-1:2013, there are many types of welded joints for steel pipes, but the most common for butt-welding two pipes is a single-sided weld with beveled edges. Incoming inspection requires assessing the quality of welded joints. Mechanical property evaluation is performed according to ISO 5177:1981, along with non-destructive testing using ultrasonic and radiographic methods. Mechanical testing includes static uniaxial tensile tests and hardness measurements (3). Continuous condition monitoring is also a common quality control method (4-6).

Standardized hardness testing methods include Brinell (7), Rockwell (8), and Vickers (9). Additionally, the instrumented indentation method has been used in many studies (10-12) to assess elastic-plastic properties. However, these methods cannot be applied for in-field pipeline inspections due to the need of specimen preparation.

A solution to this problem is the use of portable hardness testers. Among portable devices, testers with transducers implementing the Leeb dynamic method and the UCI method are the most common.

The Leeb dynamic method measures the ratio of rebound velocity to impact velocity of an indenter fixed to a striker that hits the inspected surface with a defined energy. Portable Leeb hardness testers are widely used for technical diagnostics, as regulated by ISO 16859-1:2015. Successful applications of Leeb testers for welded joint hardness control are described in (13, 14). However, Leeb method results depend on the mass, thickness, and stiffness of the tested object (15).

Thus, portable UCI hardness testers (DIN 50159-1 (2022) have gained widespread use for pipeline weld inspections. This method is based on changes in the vibration frequency of a rod with a Vickers diamond indenter upon penetration into the material, increasing the oscillation frequency (16). The frequency shift is proportional to the indentation depth, and hardness is calculated using a calibration curve. This method is successfully applied in various industries, particularly for in-service pipeline and weld inspections, due to its simplicity and sufficient accuracy for homogeneous materials. Examples include hardness testing of aerospace materials (17), fatigue properties of marine structures (18), and corrosion damage assessment in slug

catcher vessels (19). However, its primary application is in evaluating welded joint strength, including hardness mapping of weld and HAZ regions (20-23), weld defect detection (20, 24), fatigue endurance assessment for different welding techniques (21, 25, 26), and HAZ hardness distribution analysis (27-29).

A major limitation of UCI testers is their dependence on the material's elastic properties. The method assumes a uniform elastic modulus across the inspected area, matching that of the calibration specimens. If the actual modulus differs from the reference value hardness measurements will be distorted.

This issue arises in pipeline weld inspections, where welding alters the microstructure and mechanical properties (30). The results of many researches (31, 32) demonstrate that the intense thermal cycle induces structural transformations, such as martensite formation, resulting in a substantial hardness gradient between the base metal, HAZ, and the weld. Thus, a variation in the elastic modulus is observed, driven by the development of residual stresses and the heterogeneity of the material's elastic properties. These alterations critically affect the load-bearing capacity and service life of the structure, underscoring the necessity for precise control and prediction of mechanical properties post-welding. The HAZ exhibits microstructural changes due to thermal effects, influenced by steel composition, grain size, and welding parameters (33). These variations lead to UCI hardness measurement errors. Introducing a correction factor accounting for elastic modulus changes in the HAZ can improve accuracy of UCI method.

Elastic non-uniformity in the HAZ due to microstructural changes can be assessed by measuring ultrasonic (US) wave velocity, as longitudinal (cl) and transverse (cp) wave speeds depend on elastic properties. Ultrasonic attenuation is influenced by microstructural changes (34-37), though wave velocity may vary due to weld anisotropy, complicating microstructure correlations (38-40). However, studies (41-43) show that US wave velocity depends not only on microstructure but also on surface hardness in the weld and HAZ, confirming that elastic non-uniformity can be accounted for via US wave analysis to derive a UCI transducer correction.

According to regulatory documents, a welded joint is deemed non-conforming if its hardness increases by 50 HB relative to the base metal. However, as previously emphasized, the results of hardness measurements are significantly influenced by the heterogeneity of elastic

properties in the heat-affected zone (HAZ) of the weld. Therefore, the primary objective of this study is to enhance the reliability of hardness measurements in the weld and the heat-affected zone to improve the accuracy of technical diagnostics for the condition of steel pipelines. The current study investigates longitudinal US wave velocity changes to calculate elastic modulus variations in the HAZ. A correction factor was applied to UCI hardness calculations, and results were compared with Vickers microhardness measurements.

2. MATERIALS AND METHODS

2.1. Theory When a diamond indenter vibrating at a fixed frequency penetrates a material, a sharp increase in the probe's natural oscillation frequency occurs. The process can be described as follows: as a vibrating probe of mass m with an initial stiffness k_0 penetrates the material, the system's total stiffness increases by an increment Δk . The resulting frequency shift of the probe can be expressed as:

$$\Delta f = \frac{f_0}{2k_0} \Delta k \tag{1}$$

The contact stiffness Δk can be described as follows (44):

$$\Delta k \approx \frac{2}{\sqrt{\pi}} E^* \sqrt{A_c} \tag{2}$$

where A_c is the projected contact area of the indenter at the penetration depth, and E_r is the reduced elastic modulus.

The reduced elastic modulus accounts for the elastic contact between the indenter and the material (45):

$$\frac{1}{E^*} = \frac{(1-\nu^2)}{E} + \frac{(1-\nu_i^2)}{E_i} \tag{3}$$

where ν and ν_i are the Poisson's ratios of the material and indenter, respectively, and E and E_i are the elastic moduli of the material and indenter, respectively.

Substituting Equation 2 into Equation 1 and expressing A_c in terms of Vickers hardness $HV_{Vickers}$, indentation load P , and eliminating transducer-specific constants, the UCI-measured hardness becomes proportional to the elastic modulus:

$$HV_{UCI} \sim P \left(\frac{E}{\Delta f \cdot (1-\nu^2)} \right)^2 \tag{4}$$

In practice, HV_{UCI} is not calculated from Equation (4) but derived from a calibration curve $HV_{UCI}(\Delta f)$, as the actual elastic modulus of the material cannot be directly determined by this method. Calibration is performed using reference blocks with certified hardness values. The resulting calibration curve (Figure 1) is used to calculate the material's hardness.

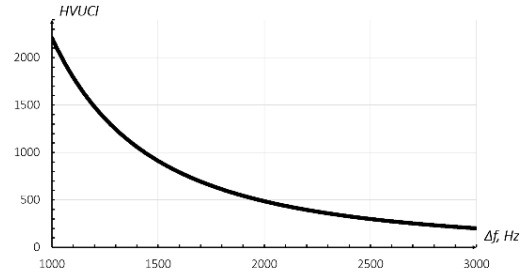


Figure 1. Calibration curve HV_{UCI} vs. Δf (16)

Since Equation 4 shows that HV_{UCI} is directly proportional to E^2 and inversely proportional to Δf^2 . Due to that, measurements in the weld and HAZ, where E is lower than in the base material, yield underestimated HV_{UCI} values, which can be similar to hardness values in unaffected regions.

To obtain accurate hardness values ($HV_{UCI(real)}$), a correction factor must be applied:

$$HV_{UCI}^{real} = HV_{UCI}^{calib} \cdot \frac{E_{real}}{E_{calib}} \tag{5}$$

where $HV_{UCI(real)}$ and $HV_{UCI(calib)}$ are the corrected and calibration-derived hardness values, respectively, and E_{real} and E_{calib} are the actual and calibration-assumed elastic moduli.

The elastic modulus is determined ultrasonically:

$$E_{real} = V_p^2 \rho \frac{(1+\nu)(1-2\nu)}{(1-\nu)} \tag{6}$$

where V_p is the longitudinal wave velocity, ρ is the metal density.

Thus, the actual elastic modulus can be calculated by measuring longitudinal wave velocity. Substituting these values into Equation 5 yields the corrected hardness in the HAZ.

2.2. Specimen Preparation

For the study, specimens of butt-welded joints were fabricated from St3 steel (US equivalent: A284Gr.D) using automatic arc welding in accordance with ISO 9692-1:2013. Type of joint is pipe-to-pipe butt-weld one sided joint, with the use of JQ.H08MnA welding wire. The specimen dimensions were 100 × 100 mm with a thickness of 10 mm (Figure 2). The chemical composition of St3 steel, according to AISI A284Gr.D, is provided in Table 1.

After welding, specimens were ground and polished to $Ra < 0.32 \mu m$ with coolant to avoid thermal effects. Surface roughness was measured using a profilometer.

TABLE 1. Mass fraction of elements in St3 steel

C	Si	Mn	P	S	Cr	Ni	Cu
0,14-0,22	0,15-0,3	0,4-0,65	<0,04	<0,05	<0,3	<0,3	<0,3

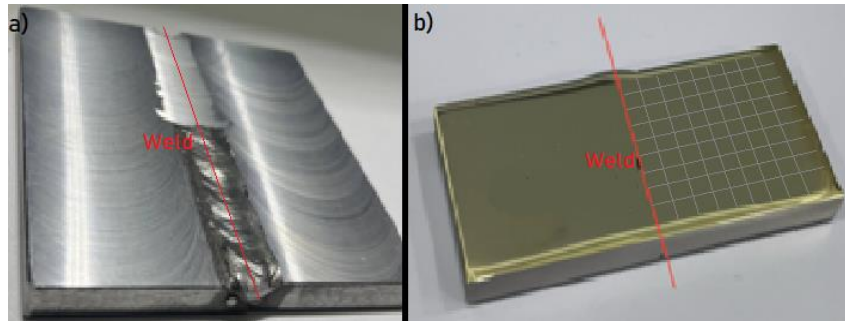


Figure 2. Test specimen: (a) after cleaning; (b) after grinding/polishing with measurement grid

2. 3. Ultrasonic Testing

Longitudinal wave velocity was measured using a UDL-2M laser-ultrasonic flaw detector. The operating principle of the UDL-2M laser-ultrasonic flaw detector is based on the laser thermo-optical generation of nanosecond ultrasonic pulses of longitudinal acoustic waves in a special broadband opto-acoustic transducer. It measures the propagation velocity of these pulses in the test specimen with one-sided transducer access. The system employs the time-of-flight measurement method. Based on the known specimen thickness and the measured time difference between the arrival of the probing ultrasonic pulse and the signal reflected from the specimen's back surface at the transducer's piezoelectric receiver, the velocity of longitudinal ultrasonic waves in the specimen is calculated.

Echo-mode measurements employed a 1–10 MHz transducer. Figure 3 shows the testing schematic.

Procedure:

1. Caliper-measured distance H from the scanning surface to the back wall.
2. A direct-contact transducer was placed on the scanning surface.
3. Time-of-flight of the backwall echo was recorded.
4. Wave velocity was calculated:

$$V_p = \frac{2H_i}{t_i} \quad (7)$$

where H_i – scanning surface-to-backwall distance at point i ; t_i – wave travel time at point i .

5. Elastic modulus was computed via Equation 5.
6. Correction factor was determined:

$$k_i = \frac{E_{real}^i}{E_{calib}} \quad (8)$$

7. Uniform density was assumed. Specimen density was derived from:

$$\rho = \frac{V}{m} \quad (9)$$

where V and m – specimen volume and mass.

8. Steps 1–6 were repeated across the measurement grid (Figure 2b) at 3 mm intervals.

2. 4. Vickers Hardness Testing

A PMT-3M microhardness tester was selected as the reference instrument for comparison with UCI results. The test load was 1.96 N (200 gf), with a dwell time of 10 seconds. Prior to testing, the indenter approach was calibrated using a halite crystal, and the built-in microscope eyepiece scale was calibrated using an objective micrometer.

Hardness measurements on both instruments followed the same indentation pattern (Figure 2b). Indentations were made from the weld centerline to the edge of the specimen with a step of 2.35 mm. Lines parallel and perpendicular to the weld were marked on the specimen with the same spacing. Hardness measurements were taken at each node of the grid. The results obtained from indentations along the same line parallel to the weld were averaged, and the resulting value was taken as the mean hardness at a specific distance from the weld. An example of an indentation imprint is shown in Figure 4. A schematic representation of the experimental setup is shown on Figure 5.

2. 5. UCI Hardness Testing

Hardness measurements were performed using a portable Konstanta KT hardness tester equipped with a UCI transducer. A constant test load of 50 N was applied for all measurements. The tester was pre-calibrated using a set of steel reference blocks with the following certified

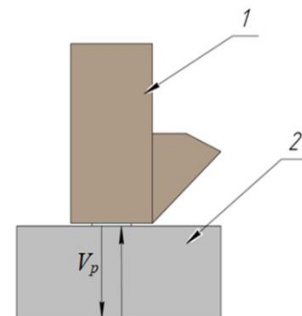


Figure 3. Longitudinal wave velocity measurement 1 – ultrasonic transducer; 2 – steel plate

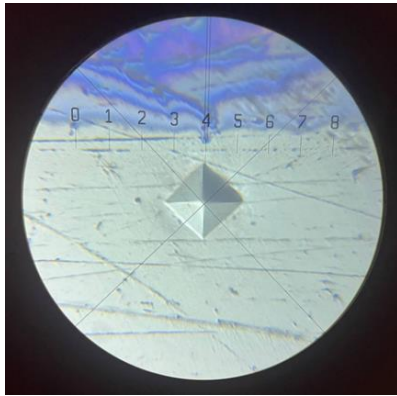


Figure 4. Example indentation

properties: $\nu = 0.27$, $E = 200$ GPa. UCI hardness measurements followed the same grid pattern as the Vickers method, but indentations were made along lines parallel to the weld between the grid nodes (Figure 2b) to avoid overlapping with prior indentation marks.

3. RESULTS AND DISCUSSION

Hardness results from both methods are shown in Figure 6.

As it can be seen, the hardness values determined by the PMT and UCI methods in the heat-affected zone (0-13 mm) do not coincide. At a distance of 2 mm from the

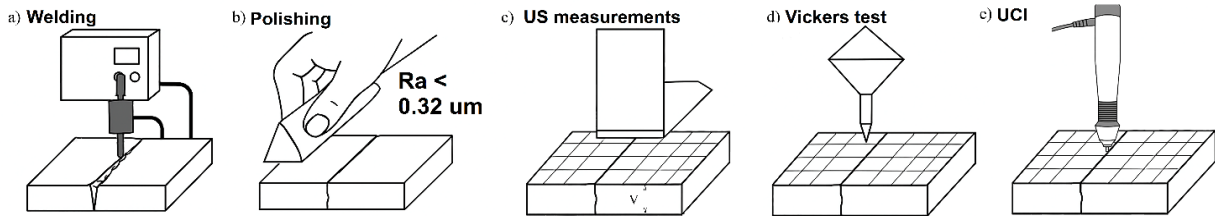


Figure 5. Experimental setup schema

weld centerline, $HV_{Vickers} = 208$ HV, while $HV_{UCI} = 188$ HV, which is nearly 10% lower than the actual hardness values. The difference in hardness values gradually decreases with increasing distance from the weld, reaching approximately 3% at 13 mm. Figure 6 also shows that beyond the transition zone (10-15 mm), the hardness values remain constant as the distance from the weld increases, confirming the capability of the UCI method to identify the boundary of the heat-affected zone. It should also be noted that beyond the heat-affected zone (>15 mm), the hardness values obtained by both methods coincide, which further supports the hypothesis about the necessity of accounting for changes in elastic properties of the material in the weld zone and HAZ when measuring hardness by the UCI method.

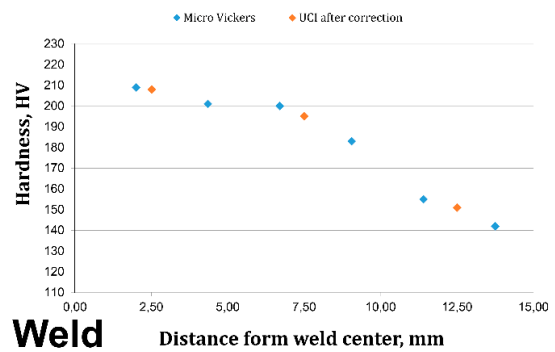


Figure 7. PMT vs. corrected UCI results

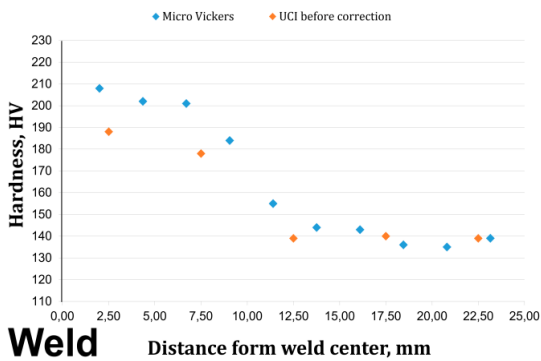


Figure 6. PMT vs. UCI results

TABLE 2. Difference between UCI and PMT results before and after correction

L, mm	Difference between UCI and PMT, HV(%)	
	Before correction	After correction
2,5	20 (9.6%)	1 (0.5%)
7,5	23 (11.4%)	5 (2.5%)
12,5	16 (10.3)	3 (1.9%)
Average	19,7 (10.4%)	3,0 (1.6%)

The measurements of longitudinal wave velocity in the weld zone and HAZ using the UDL-2M device showed values ranging from 5912 to 5984 m/s, which corresponds to an elastic modulus of 225 GPa.

Thus, it can be concluded that the actual values of the steel's elastic modulus differ from the certified values of the reference block used for transducer calibration. Additional uncertainty is introduced by the non-uniform distribution of elastic modulus values in different areas of the steel specimen. In the weld zone and at small distances from it ($L < 7$ mm), the elastic modulus values remain around 225 GPa. With increasing distance from the weld, in the HAZ the elastic modulus values gradually decrease to 220-223 GPa.

Using Equation 5 and the obtained values of E_{real} , a correction factor was calculated, and the adjusted HV_{UCI} values in the weld zone and HAZ are presented in Figure 7.

Figure 7 demonstrates that the difference between Vickers and corrected UCI hardness values is negligible in the HAZ at distances $L < 7$ mm. The average deviation between the methods is smaller than before correction (Table 2). Thus, the average difference between PMT-3 and corrected UCI hardness values is reduced to 3.0 HV (1.6%), compared to 19.7 HV (10.4%) without correction. The introduced correction improves the accuracy of UCI transducer measurements for hardness evaluation in welded joints of steel pipelines.

Currently, hardness measurements are widely used for assessing the technical condition of pipelines. Therefore, the reliability of measured hardness values is critical for ensuring safe operation. Portable hardness testing methods show potential for field monitoring systems, but this study highlights the need for additional verification of data accuracy. The deviation of the hardness value from the permissible limit must not exceed 7%. The discrepancy between the hardness values before and after the correction exceeds the allowable magnitude, which, in turn, may lead to an invalid assessment of the weld condition.

The study confirms that UCI hardness measurements are highly dependent on the match between the calibration block material and the test object. This approach is inadequate for the HAZ, where microstructural changes due to thermal effects are unaccounted for.

On the other hand, the sensitivity of elastic wave velocity to material changes under thermal exposure is reaffirmed. The elastic modulus determined ultrasonically, combined with the derived correction factor, reduced the average discrepancy between portable (UCI) and laboratory (Vickers) hardness measurements. Notably, the values nearly converge in the HAZ. These results suggest that combining ultrasonic testing with UCI can enhance the reliability of portable hardness measurements.

However, it must be noted that the extent of the HAZ and the degree of changes in physical-mechanical properties vary across steel grades. According to standards, the HAZ width can range from 1 to 4 times the

pipe wall thickness. Furthermore, studies (27, 34, 36) demonstrate that the relationship between longitudinal wave velocity, hardness, and thermal treatment depends on the steel type. An analysis of the dependence of hardness on heat treatment reveals no general correlation; even materials with similar chemical compositions exhibit different properties (46, 47). Therefore, the results of this work should be considered not from the perspective of establishing a universal correction for the elastic modulus when using the UCI method, but from the standpoint of developing a comprehensive methodology for measuring the hardness of welded joints with portable devices. Such a methodology would improve the reliability of hardness determination. The investigations carried out in this study allow for preliminary conclusions regarding the feasibility of developing such a methodology. However, further research on welded joints of various types of steel is required, which could enhance verification and validation measures for the comprehensive hardness measurement methodology.

Additionally, the 1–2% difference in wave velocity between the HAZ and base metal demands high measurement precision. In fact, this indicator can be used in designing a comprehensive hardness measurement methodology as a target for the methodology's performance criteria, namely the standard deviation characterizing repeatability, reproducibility, intermediate precision, etc. Therefore, additional metrological analysis of the possibility of ensuring the required measurement accuracy in field conditions is necessary. At the same time, as a preliminary metrological analysis, it is possible to consider, as reference values, the works in which an evaluation of the measurement uncertainty for thickness by the ultrasonic method was performed (48-53), since, in fact, measuring the speed is the inverse problem of this measurement. The analysis of (48-53) showed that with a certain approach, it is possible to ensure a thickness measurement error in the micrometer range, which exceeds the requirements for ensuring a speed measurement error of 1-2%. Furthermore, (50, 53) describe thickness measurement techniques without preliminary calibration of the elastic wave propagation velocity, based on the laws of geometrical acoustics, which is important in the context of developing a comprehensive hardness measurement methodology.

4. CONCLUSION

Addressing these aspects will generalize the findings of this study and improve the reliability of portable hardness testing methods. Main findings of the study are:

1. The accuracy of UCI hardness measurements depends significantly on the ratio between the actual elastic modulus and that of the calibration block, leading to incorrect hardness values in the HAZ.

2. Before correction, the difference between UCI and PMT hardness values in the HAZ was ~10%, a statistically significant deviation. After correction, the discrepancy is virtually eliminated.

3. Ultrasonic-based corrections for the elastic modulus improve the reliability of UCI hardness measurements in the HAZ.

Acknowledgements

The author appreciates Engineering and Design Center for Spacecraft Operation Support for providing necessary facilities to conduct present research.

Funding

This work received no funding.

Ethics Approval and Consent to Participate

This article does not involve any studies with human participants or animals performed by any of the authors. Therefore, ethics approval and consent to participate are not applicable.

Competing Interests

The author declares no financial or organizational conflicts of interest.

Data Availability

The data supporting the findings of this study are available from the corresponding author upon reasonable request.

Declaration of Generative AI and AI-assisted Technologies in the Writing Process

During the preparation of this manuscript, the author used ChatGPT exclusively for minor language editing and stylistic refinement to improve clarity and readability. The author carefully reviewed, revised, and approved the final content and takes full responsibility for the accuracy, integrity, and originality of the work. The author declares that there are no known financial or organizational conflicts of interest that could have influenced the work reported in this paper.

Author Biosketch

Dmitrii Gromyka is an Assistant professor of metrology, instrument engineering and quality control department in Saint-Petersburg mining university. He received his PhD in 2023 in Geotechnology. Main scientific interests are assessing of fatigue damage with instrumental nanoindentation.

Alexander Shikhov is an Assistant professor of metrology, instrument engineering and quality control department in Saint-Petersburg mining university. He received his PhD in 2022 in Geotechnology. Main scientific interests are the use of ultrasound nondestructive testing to evaluate mechanical properties of soils.

Alexander Umanskii is a Head of metrology, instrument engineering and quality control department in Saint-Petersburg mining university. He received his PhD in 2018 in Geotechnology. Main scientific interests are design of portable hardness testers and enhancing of their metrological properties.

Darya Kopytina is a post-graduate student of metrology, instrument engineering and quality control department in Saint-Petersburg mining university. Main scientific interests are assessing the state of PE pipes with ultrasound NDT testers.

Dinara Shakirzyanova is a post-graduate student of metrology, instrument engineering and quality control department in Saint-Petersburg mining university. Main scientific interests are evaluation of mechanical properties of steel pipes with portable hardness testers.

Shmakov Alexey is a post-graduate student of system control and robotics department of ITMO university. Main scientific interests are designing of portable nondestructive testing devices.

REFERENCES

1. Dzhemilev ER, Shammazov IA, Sidorkin DI, Mastobaev BN, Gumerov AK. Developing technology and device for the main pipelines repair with cutting out their defective sections. *Neftyanoe Khozyaystvo. Oil Industry*. 2022;2022(10):78–82. <https://doi.org/10.24887/0028-2448-2022-10-78-82>
2. Bolobov VI, Popov GG. Methodology for testing pipeline steels for resistance to grooving corrosion. *Journal of Mining Institute*. 2021;252(6):854–60. <https://doi.org/10.31897/PMI.2021.6.718-09>
3. Schipachev AM, Vardanyan ES, Mukamadeev VR, Mukamadeev IR. Investigation of changes in the surface hardness of coated cutting tools. *Metallrobrabotka*. 2021;3(123):22–29. <https://doi.org/10.25960/mo.2021.3.22>
4. Yujra RE, Vyacheslavov AV, Gogolinskiy KV, Sapozhnikova K, Taymanov R. Deformation Monitoring Systems for Hydroturbine Head-Cover Fastening Bolts in Hydroelectric Power Plants. *Sensors*. 2025;25:2548. <https://doi.org/10.3390/s25082548>
5. Krizskii VN, Kosarev OV, Aleksandrov PN, Luntovskaya YA. Mathematical modeling of the electric field of an in-line diagnostic probe of a cathode-polarized pipeline. *Journal of Mining Institute*. 2024;265:156–64.
6. Botyan E, Lavrenko S, Pushkarev A. Evaluation of Complicated Mining Exploitation Conditions Influence on Service Life of Open Pit Trucks Suspensions with Remote Monitoring Systems. *International Journal of Engineering Transactions B: Applications*. 2024;37(11):2268–75. <https://doi.org/10.5829/ije.2024.37.11b.12>
7. Zandinava B, Bakhtiari R, Vukelic G. Failure analysis of a gas transport pipe made of API 5L X60 steel. *Engineering Failure*

- Analysis. 2021;131:105881. <https://doi.org/10.1016/j.engfailanal.2021.105881>
8. Elkhodbia M, Gadala I, Barsoum I, AlFantazi A, Abdel Wahab M. Multi-physics microstructural modeling of a carbon steel pipe failure in sour gas service. *Engineering Failure Analysis*. 2025;174:109469. <https://doi.org/10.1016/j.engfailanal.2025.109469>
 9. Li L, Yu T, Xia J, Gao Y, Han B, Gao Z. Failure analysis of L415/316L composite pipe welded joint. *Engineering Failure Analysis*. 2024;158:107981. <https://doi.org/10.1016/j.engfailanal.2024.107981>
 10. Pham TH, Kim SE. Microstructure evolution and mechanical properties changes in the weld zone of a structural steel during low-cycle fatigue studied using instrumented indentation testing. *International Journal of Mechanical Sciences*. 2016;114:141–56. <https://doi.org/10.1016/j.ijmecsci.2016.05.021>
 11. Midawi A, Simha CHM, Gerlich A. Assessment of yield strength mismatch in X80 pipeline steel welds using instrumented indentation. *International Journal of Pressure Vessels and Piping*. 2018;168. <https://doi.org/10.1016/j.ijpvp.2018.09.014>
 12. Vinogradova AA, Gogolinskiy KV, Shchiptsova EK. A study of applicability of instrumented indentation method to determine the mechanical properties of thermoplastic. *Industrial laboratory. Diagnostics of materials*. 2025;91(5):67–76. <https://doi.org/10.26896/1028-6861-2025-91-5-67-76>
 13. Purnomo E, Wiranata A, Aan D, Muflikhun M. Microstructural and Mechanical Characterization of U-Bend Economizer Failures: Integrating Experimental Testing and CFD Simulation. *Journal of Materials Research and Technology*. 2025;36. <https://doi.org/10.1016/j.jmrt.2025.04.178>
 14. Li D, Hu S, Liu X, Xie Y, Feng C. Safety Performance Assessment Strategies of P91 Steel Based on Leeb Hardness. *IOP Conference Series: Earth and Environmental Science*. 2019;295:032096. <https://doi.org/10.1088/1755-1315/295/3/032096>
 15. Seijiro M, Takashi Y. Computer Simulation of Micro Rebound Hardness Test. *Procedia Engineering*. 2014;81:1396–401. <https://doi.org/10.1016/j.proeng.2014.10.163>
 16. Gogolinskii KV, Syasko VA, Umanskii AS, Nikazov AA, Bobkova TI. Mechanical properties measurements with portable hardness testers: advantages, limitations, prospects. *Journal of Physics: Conference Series*. 2019;1384:012012. <https://doi.org/10.1088/1742-6596/1384/1/012012>
 17. Gvozdyakov DV, Zenkov AV, Gubin VE, Kaltaev AZh, Marysheva YaV. Experimental studies into the effect of air pressure on the atomization characteristics of coal-water slurries. *iPolytech Journal*. 2021;25(5):586–600. https://doi.org/10.52351/00260827_2021_09_81
 18. Corigliano P, Crupi V, Fricke W, Friedrich N, Guglielmino E. Experimental and numerical analysis of fillet-welded joints under low-cycle fatigue loading by means of full-field techniques. *Proceedings of the Institution of Mechanical Engineers, Part C: Journal of Mechanical Engineering Science*. 2015;229. <https://doi.org/10.1177/0954406215571462>
 19. Jasim AH, Nuha H, Khanjar A. Investigation of slug catcher vessel degradation by hydrogen sulfide (H₂S) damage. *Heliyon*. 2024;10:e40307. <https://doi.org/10.1016/j.heliyon.2024.e40307>
 20. Voelkel J, Meissner M, Bartsch H, Feldmann M. The influence of external weld imperfection size on the load-bearing capacity of butt-welded joints. *Journal of Constructional Steel Research*. 2024;220:108808. <https://doi.org/10.1016/j.jcsr.2024.108808>
 21. Churiaque C, Sánchez-Amaya J, Üstündag Ö, Porrúa-Lara M, Gumenyuk A, Rethmeier M. Improvements of hybrid laser arc welding for shipbuilding T-joints with 2F position of 8 mm thick steel. *Optics & Laser Technology*. 2021;143:107284. <https://doi.org/10.1016/j.optlastec.2021.107284>
 22. Üstündag Ö, Bakir N, Gumenyuk A, Rethmeier M. Improvement of Charpy impact toughness by using an AC magnet backing system for laser hybrid welding of thick S690QL steels. *Procedia CIRP*. 2022;111:462–65. <https://doi.org/10.1016/j.procir.2022.08.067>
 23. Schroepfer D, Witte J, Kromm A, Kannengiesser T. Stresses in repair welding of high-strength steels—part 2: heat control and stress optimization. *Welding in the World*. 2024;68. <https://doi.org/10.1007/s40194-024-01731-7>
 24. Rhode M, Erleben K, Richter T, Schroepfer D, Mente T, Michael T. Local mechanical properties of dissimilar metal TIG welded joints of CoCrFeMnNi high entropy alloy and AISI 304 austenitic steel. *Welding in the World*. 2024;68:1–11. <https://doi.org/10.1007/s40194-024-01718-4>
 25. Fuštar B, Lukačević I, Skejić D, Garašić I. Fatigue tests of S690 as-welded and HFMI-treated details with longitudinal and transverse attachments. *Results in Engineering*. 2024;23:1–8. <https://doi.org/10.1016/j.rineng.2024.102386>
 26. Diekhoff P, Hensel J, Nitschke-Pagel T, Dilger K. Investigation on fatigue strength of cut edges produced by various cutting methods for high-strength steels. *Welding in the World*. 2020;64. <https://doi.org/10.1007/s40194-020-00853-y>
 27. Schroeder N, Rhode M, Kannengiesser T. Thermodynamic prediction of precipitations behaviour in HAZ of a gas metal arc welded S690QL with varying Ti and Nb content. *Welding in the World*. 2023;67. <https://doi.org/10.1007/s40194-023-01550-2>
 28. Brätz O, von Armin M, Eichler S, Gericke A, Henkel K-M, Hildebrand J, Bergmann J, Kuhlmann U. Load-carrying capacity of MAG butt and fillet welded joints on high-strength structural steels of grade S960QL and S960MC. *CE/Papers*. 2023;6:587–94. <https://doi.org/10.1002/cepa.2478>
 29. Churiaque C, Sánchez-Amaya JM, Porrúa-Lara M, Gumenyuk A, Rethmeier M. The effects of HLAW parameters for one side T-joints in 15 mm thickness naval steel. *Metals*. 2021;11(4):600. <https://doi.org/10.3390/met11040600>
 30. Pryakhin EI, Sharapova DM. Understanding the structure and properties of the heat affected zone in welds and model specimens of high-strength low-alloy steels after simulated heat cycles. *CIS Iron and Steel Review*. 2020;19:60–65. <https://doi.org/10.17580/cisirs.2020.01.12>
 31. Rahmani M, Moslemi Petrudi A. Investigation of crack growth by loading fatigue due to fluid and structural coupling vibrations in the joint of thermowell welding in gas pipeline. *Journal of Research in Engineering and Applied Sciences*. 2020;5(2):28–37. <https://doi.org/10.46565/jreas.2020.v05i02.001>
 32. Mičian M, Winczek J, Gucwa M, Koňár R, Málek M, Postawa P. Investigation of welds and heat affected zones in weld surfacing steel plates taking into account the bead sequence. *Materials*. 2020;13:5666. <https://doi.org/10.3390/ma13245666>
 33. Sizyakov MI. The use of steel arc welding pipes on tank farms or oil and gas industry objects. *Petroleum Engineering*. 2020;18:88–93. <https://doi.org/10.17122/ngdelo-2020-2-88-93>
 34. Kalimuthu V, Muthupandi V, Jayachitra R. Influence of heat treatment on the microstructure, ultrasonic attenuation and hardness of SAF 2205 duplex stainless steel. *Materials Science and Engineering: A*. 2011;529:447–51. <https://doi.org/10.1016/j.msea.2011.09.059>
 35. Mutlu I, Oktay E, Ekinci S. Characterization of microstructure of H13 tool steel using ultrasonic measurements. *Russian Journal of Nondestructive Testing*. 2013;49. <https://doi.org/10.1134/S106183091302006X>
 36. Borovkov AI, Prokhorovich VE, Bychenok VA, Berkutov IV, Alifanova IE. Ultrasonic inspection technique for welded joints obtained by spot friction stir welding. *Russian Journal of Nondestructive Testing*. 2023;59(2):149–60. <https://doi.org/10.1134/S1061830923700262>

37. Shikhov A, Gogolinsky K, Zubarev A, Smorodinsky Ya, Kopytina D, Vinogradova A. Analysis of the requirements for metrological support of methods and means of ultrasound control. *Russian Journal of Nondestructive Testing*. 2025;61(3):1061–69. <https://doi.org/10.1134/S1061830924603180>
38. Carreón H, Barrera G, Natividad C, Salazar M, Contreras A. Relation between hardness and ultrasonic velocity on pipeline steel welded joints. *Nondestructive Testing and Evaluation*. 2015;31(2):97–108. <https://doi.org/10.1080/10589759.2015.1074231>
39. Bolobov VI, Latipov IU, Zhukov VS, Popov GG. Using the magnetic anisotropy method to determine hydrogenated sections of a steel pipeline. *Energies*. 2023;16:5585. <https://doi.org/10.3390/en16155585>
40. Bychenok VA, et al. Ultrasonic testing of adhesion of special coatings. *Russian Journal of Nondestructive Testing*. 2023;59(8):839–46. <https://doi.org/10.1134/S1061830923700481>
41. Carreon M, Ruiz A, Medina A, Barrera Cardiel G, Zárate MJ. Characterization of the alumina–zirconia ceramic system by ultrasonic velocity measurements. *Materials Characterization*. 2009;60:875–81. <https://doi.org/10.1016/j.matchar.2009.02.008>
42. Daqing W, Yajie W, Weihua L, Chen H, Chun Y, Hao L. Multiscale investigation of microstructure optimization in the arc additive manufacturing and arc welding by self-induced ultrasound. *International Journal of Heat and Mass Transfer*. 2021;180:121790. <https://doi.org/10.1016/j.ijheatmasstransfer.2021.121790>
43. Cécile G, Jean M, Marie-Aude P, Gilles C, Bertrand C. Influence of the uncertainty of elastic constants on the modelling of ultrasound propagation through multi-pass austenitic welds. Impact on non-destructive testing. *International Journal of Pressure Vessels and Piping*. 2019;171:125–36. <https://doi.org/10.1016/j.ijpvp.2019.02.011>
44. Fischer-Cripps AC. *Introduction to contact mechanics*. 2nd ed. US: Springer; 2007. p. 226.
45. Oliver W, Pharr G. An improved technique for determining hardness and elastic modulus using load and displacement sensing indentation experiments. *Journal of Materials Research*. 1992;7(6):1564–83. <https://doi.org/10.1557/JMR.1992.1564>
46. Bharare OS, Sarve SA, Gengane VV, Sahane AS, Jikar PC. Effect of various surface heat treatment methods and its parametric variation on the hardness properties of different steels grades. *Materials Today: Proceedings*. 2024;102:132–39. <https://doi.org/10.1016/j.matpr.2023.04.057>
47. Anggraini L, Kartomi H. Hot forgeability of SCR420 low-alloy steel for piston rod application. In: *Journal of Physics: Conference Series*. 2020;1595(1):012007. <https://doi.org/10.1088/1742-6596/1595/1/012007>
48. Wangyu L, Dongxun L, Weigui X. A novel time-of-flight difference determination method for ultrasonic thickness measurement with ultrasonic echo onset point detection. *Applied Acoustics*. 2025;233:110605. <https://doi.org/10.1016/j.apacoust.2025.110605>
49. Peng Z, Shijie W, Pan D, Xinru G, Tonghai W, Min Y, Yaguo L. High-accuracy ultrasonic measurement of oil film thickness in sliding bearings considering surface thin coating. *Tribology International*. 2025;110343. <https://doi.org/10.1016/j.triboint.2024.110343>
50. Pan D, Laisheng Z, Tonghai W, Min Y, Tom R, Zhongxiao P. Simultaneous measurement of thickness and sound velocity of porous coatings based on the ultrasonic complex reflection coefficient. *NDT & E International*. 2022;131:102683. <https://doi.org/10.1016/j.ndteint.2022.102683>
51. Hao C, Kaipeng J, Wei Z, Chengqian Z, Jianzhong F, Peng Z. High precision ultrasonic measurement method for thin-walled parts. *NDT & E International*. 2024;145:103122. <https://doi.org/10.1016/j.ndteint.2024.103122>
52. Morana M, Damir M, Biserka R, Zdenka K. Measurement uncertainty evaluation of ultrasonic wall thickness measurement. *Measurement*. 2019;137:179–88. <https://doi.org/10.1016/j.measurement.2019.01.027>
53. Marcelo YM, Nicolás P, Flávio B, Julio CA, Marcos SGT. Error analysis of self-compensated ultrasound measurements of the thickness loss due to corrosion in pipe walls. *Ultrasonics*. 2024;142:107387. <https://doi.org/10.1016/j.ultras.2024.107387>

COPYRIGHTS

©2026 The author(s). This is an open access article distributed under the terms of the Creative Commons Attribution (CC BY 4.0), which permits unrestricted use, distribution, and reproduction in any medium, as long as the original authors and source are cited. No permission is required from the authors or the publishers.



Persian Abstract

چکیده

کنترل کیفیت اتصالات جوش داده شده شامل اندازه گیری سختی هر دو جوش و ناحیه متأثر از حرارت (HAZ) است. با این حال، روش های استاندارد تست سختی نیاز به آماده سازی نمونه دارد که منجر به خرابی خط لوله می شود. در میان دستگاه های قابل حمل، سختی سنج ها با استفاده از روش امپدانس تماس اولتراسونیک (UCI) بیشترین استفاده را دارند. با این حال، نتایج اندازه گیری به منحنی کالیبراسیون بستگی دارد، که خواص الاستیک نمونه را به حساب می آورد و یکنواختی آنها را در کل سطح بازرسی شده فرض می کند. در HAZ یک اتصال جوش داده شده، تغییراتی در ریزساختار و خواص الاستیک فلز رخ می دهد که منجر به خطاهای اندازه گیری در تست سختی UCI می شود. این مقاله روشی را برای اعمال تصحیح در کالیبراسیون با در نظر گرفتن تغییرات واقعی در مدول الاستیک در HAZ، که از طریق نظارت بر سرعت موج اولتراسونیک اندازه گیری می شود، ارائه می کند. در نتیجه، مقادیر سختی که این تصحیح را شامل می شوند، مطابقت بهتری با نتایج مرجع به دست آمده با استفاده از تستر میکروسختی ویکرز نشان دادند، که نشان می دهد اصلاح پیشنهادی دقت اندازه گیری مبدل UCI را بهبود می بخشد.